

Siberian Branch of Russian Academy of Science
BUDKER INSTITUTE OF NUCLEAR PHYSICS

V.N. Baier and V.M. Katkov

THE LANDAU-POMERANCHUK-MIGDAL EFFECT
AND TRANSITION RADIATION
IN STRUCTURED TARGETS

Budker INP 99-13

NOVOSIBIRSK
1999

**The Landau-Pomeranchuk-Migdal effect
and transition radiation
in structured targets**

V.N. Baier and V.M. Katkov

Budker Institute of Nuclear Physics
630090 Novosibirsk, Russia

Abstract

The radiation from high-energy electrons is investigated for the case when a target consists of several separated plates. The spectrum of radiation is considered in the region in which the bremsstrahlung is under influence of the multiple scattering of a projectile (the LPM effect), the polarization of a medium and the hard part of the boundary radiation contribute. In this region the general expression for the radiation spectrum is obtained for the N -plate target. A qualitative description of the arising interference pattern is given.

1 Introduction

The process of bremsstrahlung from high-energy electron occurs over a rather long distance, known as the formation length. If the formation length of the bremsstrahlung becomes comparable to the distance over which a mean angle of multiple scattering becomes comparable with a characteristic angle of radiation, the bremsstrahlung will be suppressed (the Landau-Pomeranchuk-Migdal (LPM) effect [1], [2]). An influence of polarization of a medium on radiation process leads also to suppression of the soft photon emission (Ter-Mikaelian effect, see in [3]).

A very successful series of experiments [4] - [6] was performed at SLAC during recent years. In these experiments the cross section of the bremsstrahlung of soft photons with energy from 200 keV to 500 MeV from electrons with energies 8 GeV and 25 GeV is measured with an accuracy of the order of a few percent. Both the LPM effect, and dielectric suppression (the effects of the polarization of a medium) were observed and investigated. These experiments were a challenge for a theory since in all the previous papers calculations (cited in [7]) were performed to logarithmic accuracy which is not enough for a description of the new experiment.

Very recently authors developed the new approach to the theory of the LPM effect [7] in which the cross section of the bremsstrahlung process in the photon energies region where the influence of the LPM is very strong was calculated with a term $\propto 1/L$, where L is characteristic logarithm of the problem, and with the Coulomb corrections taken into account. In the photon energy region, where the LPM effect is "turned off", the obtained cross section gives the exact Bethe-Heitler cross section (within power accuracy) with the Coulomb corrections. This important feature was absent in the previous calculations. The polarization of a medium is incorporated into this approach. The considerable contribution into the soft part of the measured spectrum of radiation gives a photon emission on the boundaries

of a target. In [7] we investigated the case when a target is much thicker or much thinner than the formation length of the radiation. A target of an intermediate thickness was studied in paper [8]. In the last paper we derived general expression for the spectral probability of radiation in a thin target and in a target of intermediate thickness in which the multiple scattering, the polarization of a medium and radiation on the boundaries of a target are taken into account. In [9] the effect of multiphoton emission from a single electron was studied, this effect is very essential for understanding data [4]-[6]. The LPM effect was recently under active investigation, see e.g. [10], [11] and review [12].

In papers [7], [8] the target is considered as a homogeneous plate. A radiator which consists of a set of thin plates is of great interest.

The radiation from several plates for the relatively hard part of the spectrum in which the bremsstrahlung in the condition of the strong LPM effect dominates was investigated recently in [13]. A rather curious interference pattern in the spectrum of the radiation was found which depends on a number (and a thickness) of plates and the distance between plates. In this part of the spectrum one can neglect the effects of the polarization of a medium.

In the present paper the probability of radiation in a radiator consisting of N plates is calculated. The transition radiation dominates in the soft part of the considered spectrum, while the bremsstrahlung under influence of the strong LPM effect dominates in the hard part. The intermediate region of the photon energies where contributions of the both mentioned mechanisms are of the same order is of evident interest. We consider this region in detail. In this region effects of the polarization of the medium are essential. The numerical calculation was performed for the radiator of two gold plates with thickness $l_1 = 0.35\% L_{rad}$, L_{rad} is the radiation length, (the same object was considered in [13]). The interference pattern depending on the distance between plates was analyzed in the intermediate region. An another interference pattern was found in the soft part of the spectrum where the transition radiation contributes only.

2 Radiation from structured target

With allowance for the multiple scattering and the polarization of a medium we have for the spectral distribution of the probability of radiation (see

Eq.(4.4) of [7],and Eq.(2.1) of [8])

$$\begin{aligned} \frac{dw}{d\omega} &= \frac{4\alpha}{\omega} \text{Re} \int_{-\infty}^{\infty} dt_2 \int_{-\infty}^{t_2} dt_1 \exp\left(-i \int_{t_1}^{t_2} \mu(t) dt\right) \\ &\times \langle 0 | r_1 S(t_2, t_1) + r_2 \mathbf{p} S(t_2, t_1) \mathbf{p} | 0 \rangle, \end{aligned} \quad (2.1)$$

where

$$\begin{aligned} \mu(t) &= 1 + \kappa_0^2 g(t), \quad t = \frac{l}{l_0}, \quad l_0 = \frac{2\varepsilon\varepsilon'}{\omega m^2}, \\ r_1 &= \frac{\omega^2}{\varepsilon^2}, \quad r_2 = 1 + \frac{\varepsilon'^2}{\varepsilon^2}, \quad \kappa_0 = \frac{\omega_p}{\omega}, \\ \omega_p &= \gamma\omega_0, \quad \gamma = \frac{\varepsilon}{m}, \quad \omega_0^2 = \frac{4\pi\alpha n}{m}, \end{aligned} \quad (2.2)$$

here ε is the energy of the initial electron, ω is the energy of radiated photon, $\varepsilon' = \varepsilon - \omega$, n is the density of electrons in a medium, l is the length of the trajectory of a particle, the function $g(t)$ describes change of the density of a medium on the trajectory. The mean value in Eq.(2.1) is taken over states with definite value of the two-dimensional operator $\boldsymbol{\varrho}$ (see [7], Section 2). The propagator of electron has a form

$$S(t_2, t_1) = \text{T exp} \left[-i \int_{t_1}^{t_2} \mathcal{H}(t) dt \right], \quad (2.3)$$

where the Hamiltonian $\mathcal{H}(t)$ is

$$\begin{aligned} \mathcal{H}(t) &= \mathbf{p}^2 - iV(\boldsymbol{\varrho})g(t), \quad \mathbf{p} = -i\nabla_{\boldsymbol{\varrho}}, \\ V(\boldsymbol{\varrho}) &= Q\boldsymbol{\varrho}^2 \left(L_1 + \ln \frac{4}{\boldsymbol{\varrho}^2} - 2C \right), \quad Q = \frac{2\pi Z^2 \alpha^2 \varepsilon \varepsilon' n}{m^4 \omega}, \quad L_1 = \ln \frac{a_s^2}{\lambda_c^2}, \\ \frac{a_s^2}{\lambda_c} &= 183 Z^{-1/3} e^{-f}, \quad f = f(Z\alpha) = (Z\alpha)^2 \sum_{k=1}^{\infty} \frac{1}{k(k^2 + (Z\alpha)^2)}, \end{aligned} \quad (2.4)$$

where $C = 0.577216\dots$ is Euler's constant. The contribution of scattering of a projectile on the atomic electrons may be incorporated into the effective potential $V(\boldsymbol{\varrho})$. The summary potential including both an elastic and an inelastic scattering is

$$V(\boldsymbol{\varrho}) + V_e(\boldsymbol{\varrho}) = -Q_{ef} \boldsymbol{\varrho}^2 \left(\ln \frac{\lambda_c^2}{a_{ef}^2} + \ln \frac{\boldsymbol{\varrho}^2}{4} + 2C \right), \quad (2.5)$$

where

$$Q_{ef} = Q\left(1 + \frac{1}{Z}\right), \quad a_{ef} = a_{s2} \exp\left[\frac{1.88 + f(Z\alpha)}{1 + Z}\right].$$

In Eq.(2.1) it is implied that the subtraction is made at $V = 0$, $\kappa = 1$.
In [8] the target was one plate of an arbitrary thickness l_1

$$g(t) = \vartheta(t)\vartheta(T_1 - t), \quad T_1 = l_1/l_0$$

Here we consider the case when the target consists of N identical plates of thickness l_1 with the equal gaps l_2 between them. The case $l_1 \ll l_c$ will be analyzed where l_c is the characteristic formation length of radiation in absence of a matter ($\kappa_0 = 0$)

$$l_c = \frac{l_0}{1 + \gamma^2 \vartheta_c^2} = \frac{l_0}{1 + p_c^2}, \quad \frac{l_1}{l_c} = (1 + p_c^2)T_1 \ll 1, \quad (2.6)$$

where ϑ_c is the characteristic angle of radiation.

In [7] (Sect.5) we obtained the following expression for the operator $S(t_2, t_1)$

$$S(t_2, t_1) = \exp(-iH_0 t_2) T \exp\left[-\int_{t_1}^{t_2} V(\mathbf{q} + 2\mathbf{p}t, t) dt\right] \exp(iH_0 t_1), \quad (2.7)$$

where $H_0 = \mathbf{p}^2$, $V(\mathbf{q}, t) = V(\mathbf{q})g(t)$, T means the chronological product. Let us introduce new variables

$$t_1 = n_1 T - \tau_1, \quad t_2 = n_2 T + \tau_2 + T_1, \quad T = T_1 + T_2, \\ 0 < \tau_1 < T \quad (n_1 \geq 1), \quad 0 < \tau_2 < T \quad (n_2 \leq (N - 1)). \quad (2.8)$$

Substituting these variables into Eq.(2.7) we have

$$S(t_2, t_1) = \exp[-iH_0 (n_2 T + \tau_2 + T_1)] \quad (2.9) \\ \times \exp\left[-\int_{n_2 T}^{n_2 T + T_1} V(\mathbf{q} + 2\mathbf{p}(n_2 T + \tau)) d\tau\right] \\ \times \exp\left[-\int_{(n_2 - 1)T}^{(n_2 - 1)T + T_1} V(\mathbf{q} + 2\mathbf{p}((n_2 - 1)T + \tau)) d\tau\right] \dots \\ \times \exp\left[-\int_{n_1 T}^{n_1 T + T_1} V(\mathbf{q} + 2\mathbf{p}(n_1 T + \tau)) d\tau\right] \exp[iH_0 (n_1 T + \tau_1)]$$

Using the equality

$$V(\mathbf{q} + 2\mathbf{p}nT) = \exp(iH_0 nT) V(\mathbf{q}) \exp(-iH_0 nT) \quad (2.10)$$

and the condition (2.6) we obtain

$$S(t_2, t_1) \simeq \exp(-iH_0\tau_2) \exp(-V(\boldsymbol{\varrho})T_1) \exp(-iH_0T) \exp(-V(\boldsymbol{\varrho})T_1) \dots \exp(-iH_0T) \exp(-V(\boldsymbol{\varrho})T_1) \exp(iH_0\tau_1). \quad (2.11)$$

Here we neglected the term $-iH_0T_1$ in the exponent ($\exp(-iH_0(\tau_2 + T_1)) \rightarrow \exp(-iH_0\tau_2)$) since $H_0T_1 \sim p_c^2T_1 \ll 1$, we neglected also the term $2\mathbf{p}\tau$ in the argument of the function $V(\boldsymbol{\varrho} + 2\mathbf{p}\tau)$ (the term of the order $1/p_c$ is conserved in comparison with the term of the order p_cT_1 , see [7], Sect.5).

We will use below the matrix element of the form

$$g_n(\mathbf{p}', \mathbf{p}) = \langle \mathbf{p}' | \exp(-a(\boldsymbol{\varrho})) \exp(-iH_0T) \exp(-a(\boldsymbol{\varrho})) \dots \exp(-iH_0T) \exp(-a(\boldsymbol{\varrho})) | \mathbf{p} \rangle, \quad (2.12)$$

where $a(\boldsymbol{\varrho}) \equiv V(\boldsymbol{\varrho})T_1$, the matrix element is calculated between states with definite momentum. The potential $V(\boldsymbol{\varrho})$ in Eq.(2.4) we write in the form

$$V(\boldsymbol{\varrho}) = V_b(\boldsymbol{\varrho}) + v(\boldsymbol{\varrho}), \quad V_b(\boldsymbol{\varrho}) = q\boldsymbol{\varrho}^2, \quad q = QL_b, \\ L_b \equiv L(\varrho_b) = \ln \frac{a_s^2}{\lambda_c^2 \varrho_b^2}, \quad v(\boldsymbol{\varrho}) = -\frac{q\boldsymbol{\varrho}^2}{L} \left(\ln \frac{\boldsymbol{\varrho}^2}{4\varrho_b^2} + 2C \right), \quad (2.13)$$

where the parameter ϱ_b is defined by a set of equations (we rearranged terms in Eq.(5.9) of [7]):

$$\varrho_b = 1, \quad L_b = L_1 \quad \text{for} \quad 4QL_1T_1 = \frac{2\pi}{\alpha} \frac{l_1}{L_{rad}} \leq 1, \quad q = QL_1; \\ 4QL(\varrho_b)T_1\varrho_b^2 = \frac{2\pi}{\alpha} \frac{l_1}{L_{rad}} \varrho_b^2 \left(1 - \frac{\ln \varrho_b^2}{L_1} \right) = 1, \quad \text{for} \quad 4QL_1T_1 > 1, \quad (2.14)$$

where L_1 is defined in Eq.(2.4). The parameter $\varrho_b \simeq 1/p_c$ is determined by a characteristic angle of radiation (momentum transfer). We will calculate the matrix element $g_n(\mathbf{p}', \mathbf{p})$ in the first approximation neglecting correction terms containing $v(\boldsymbol{\varrho})$. Then

$$V(\boldsymbol{\varrho}) \simeq V_b(\boldsymbol{\varrho}) = q\boldsymbol{\varrho}^2, \quad g_1(\mathbf{p}', \mathbf{p}) = \langle \mathbf{p}' | \exp(-qT_1\boldsymbol{\varrho}^2) | \mathbf{p} \rangle \\ = \int d^2\varrho \langle \mathbf{p}' | \boldsymbol{\varrho} \rangle \langle \boldsymbol{\varrho} | \exp(-qT_1\boldsymbol{\varrho}^2) | \boldsymbol{\varrho} \rangle \langle \boldsymbol{\varrho} | \mathbf{p} \rangle \\ = \frac{1}{(2\pi)^2} \int d^2\varrho \exp [i(\mathbf{p} - \mathbf{p}')\boldsymbol{\varrho} - qT_1\boldsymbol{\varrho}^2] = \frac{b}{\pi} \exp [-b(\mathbf{p} - \mathbf{p}')^2], \quad (2.15)$$

where $b = 1/(4qT_1)$. In the calculation of the expression (2.12) we insert the combinations of the state vectors $|\mathbf{p}_1\rangle \langle \mathbf{p}_1| \dots |\mathbf{p}_{n-1}\rangle \langle \mathbf{p}_{n-1}|$ between the

operators $\exp(-a(\boldsymbol{q}))$ and use the matrix element calculated in (2.15), we have (the details of calculation are given in Appendix A)

$$\begin{aligned}
g_n(\mathbf{p}', \mathbf{p}) &= \left(\frac{b}{\pi}\right)^n \int d^2 p_1 \int d^2 p_2 \dots \int d^2 p_{n-1} \exp \left[-b (\mathbf{p}' - \mathbf{p}_1)^2 \right. \\
&\quad \left. - i\mathbf{p}_1^2 T - b (\mathbf{p}_1 - \mathbf{p}_2)^2 - i\mathbf{p}_2^2 T \dots - b (\mathbf{p}_{n-1} - \mathbf{p})^2 - i\mathbf{p}_{n-1}^2 T \right] \\
&= \frac{b}{\pi d_n} \exp \left\{ -\frac{b}{d_n} [(\mathbf{p}'^2 + \mathbf{p}^2) (d_n - d_{n-1}) - 2\mathbf{p}\mathbf{p}'] \right\}, \quad (2.16)
\end{aligned}$$

where

$$d_n \equiv d_n(\alpha) = \frac{1}{2\sqrt{\alpha^2 - 1}} \left[(\alpha + \sqrt{\alpha^2 - 1})^n - (\alpha - \sqrt{\alpha^2 - 1})^n \right], \quad \alpha = 1 + \frac{iT}{2b} \quad (2.17)$$

The obtained function $d_n(\alpha)$ is the polynomial with respect to α of degree $(n - 1)$

$$d_0 = 0, \quad d_1 = 1, \quad d_2 = 2\alpha, \quad d_3 = 4\alpha^2 - 1, \quad d_4 = 4\alpha(2\alpha^2 - 1) \dots \quad (2.18)$$

After substitution $\alpha = \cosh \eta$ we find from Eqs.(2.17) and (2.16)

$$\begin{aligned}
d_n &= \frac{\sinh n\eta}{\sinh \eta}, \quad g_n(\mathbf{p}', \mathbf{p}) = \frac{b \sinh \eta}{\pi \sinh n\eta} \exp \left\{ -\frac{b}{\sinh n\eta} \right. \\
&\quad \left. \times [(\mathbf{p}'^2 + \mathbf{p}^2) (\sinh n\eta - \sinh (n - 1)\eta) - 2 \sinh \eta \mathbf{p}\mathbf{p}'] \right\}, \quad (2.19)
\end{aligned}$$

where

$$\sinh \eta = 2\sqrt{iqT_1 T (1 + iqT_1 T)}.$$

For the case $\eta \ll 1$ one has

$$\begin{aligned}
\eta &\simeq 2\sqrt{iqT_1 T} \equiv 2T\sqrt{i\bar{q}}, \quad \bar{q} = q\frac{T_1}{T} = q\frac{l_1}{l_1 + l_2}, \\
g_n(\mathbf{p}', \mathbf{p}) &\simeq \frac{b\eta}{\pi \sinh n\eta} \exp \left\{ -\frac{b\eta}{\sinh n\eta} [(\mathbf{p}'^2 + \mathbf{p}^2) \cosh n\eta - 2\mathbf{p}\mathbf{p}'] \right\} \quad (2.20)
\end{aligned}$$

For the limiting case $n\eta \ll 1$ one has

$$g_n(\mathbf{p}', \mathbf{p}) \simeq \frac{b}{\pi n} \exp \left\{ -\frac{b}{n} (\mathbf{p}' - \mathbf{p})^2 \right\}. \quad (2.21)$$

Using the results obtained we can calculate now the mean value entering Eq.(2.1)

$$\begin{aligned}
\langle 0 | S_n(t_2, t_1) | 0 \rangle &= \int d^2 p' \int d^2 p \langle 0 | \mathbf{P}' \rangle \langle \mathbf{P}' | S_n(t_2, t_1) | 0 \rangle \langle \mathbf{P} | 0 \rangle \\
&= \frac{1}{(2\pi)^2} \int d^2 p' \int d^2 p \exp(-i\mathbf{P}'^2 \tau_2 - i\mathbf{P}^2 \tau_1) g_n(\mathbf{P}', \mathbf{P}) = \frac{b}{4\pi d_n \gamma_n}, \\
\gamma_n &= \sigma_n^2 - \beta_n^2 + i\sigma_n(\tau_1 + \tau_2) - \tau_1 \tau_2, \quad \beta_n = \frac{b}{d_n}, \quad \sigma_n = \beta_n(d_n - d_{n-1}). \quad (2.22)
\end{aligned}$$

If we use the same procedure for the second mean value in (2.1) we obtain

$$\langle 0 | \mathbf{P} S_n(t_2, t_1) \mathbf{P} | 0 \rangle = \frac{b^2}{4\pi d_n^2 \gamma_n^2}. \quad (2.23)$$

We split now the spectral distribution of the probability of radiation into two parts

$$\begin{aligned}
\frac{dw}{d\omega} &= \frac{dw_{br}}{d\omega} + \frac{dw_{tr}}{d\omega}; \\
\frac{dw_{br}}{d\omega} &= \frac{4\alpha}{\omega} \text{Re} \int_{-\infty}^{\infty} dt_2 \int_{-\infty}^{t_2} dt_1 \exp\left(-i \int_{t_1}^{t_2} \mu(t) dt\right) \\
&\times \langle 0 | r_1 \left(S(t_2, t_1) - S^{(0)}(t_2, t_1) \right) + r_2 \mathbf{P} \left(S(t_2, t_1) - S^{(0)}(t_2, t_1) \right) \mathbf{P} | 0 \rangle \quad (2.24)
\end{aligned}$$

$$\begin{aligned}
\frac{dw_{tr}}{d\omega} &= \frac{4\alpha}{\omega} \text{Re} \int_{-\infty}^{\infty} dt_2 \int_{-\infty}^{t_2} dt_1 \left[\exp\left(-i \int_{t_1}^{t_2} \mu(t) dt\right) - \exp(-i(t_2 - t_1)) \right] \\
&\times \langle 0 | r_1 S^{(0)}(t_2, t_1) + r_2 \mathbf{P} S^{(0)}(t_2, t_1) \mathbf{P} | 0 \rangle, \\
S^{(0)}(t_2, t_1) &= \exp[-iH_0(t_2 - t_1)], \quad (2.25)
\end{aligned}$$

where $dw_{br}/d\omega$ is the spectral distribution of the probability of bremsstrahlung with allowance for the multiple scattering and polarization of a medium, $dw_{tr}/d\omega$ is the probability of the transition radiation obtained in the frame of quantum electrodynamics.

Note that the subtraction in Eq.(2.24) has to follow the procedure

$$\langle 0 | S_n | 0 \rangle - \langle 0 | S_n(q=0) | 0 \rangle. \quad (2.26)$$

The integral in the exponential in (2.24) is

$$\int_{t_1}^{t_2} \mu(t) dt = \tau_1 + \tau_2 + \kappa T_1 + (n-1)\bar{\kappa}T, \quad \kappa = 1 + \kappa_0^2, \quad \bar{\kappa} = 1 + \bar{\kappa}_0^2, \quad \bar{\kappa}_0^2 = \frac{\kappa_0^2 l_1}{l_1 + l_2}, \quad (2.27)$$

where we used notations introduced in (2.2) and (2.8).

Substituting (2.22), (2.23), (2.26) and (2.27) into Eq.(2.24) we obtain the following expression for the spectral distribution of the probability of the bremsstrahlung with allowance for the multiple scattering and the polarization of a medium for the N -plate target

$$\begin{aligned} \frac{dw_{br}^{(N)}}{d\omega} &= \frac{\alpha}{\pi\omega} \operatorname{Re} \sum_{n_1, n_2=0}^{N-1} \int d\tau_2 \int d\tau_1 \exp[-i(\tau_1 + \tau_2 + \kappa T_1 + (n-1)\bar{\kappa}T)] \\ &\times [r_1 (G_n - G_n(0)) + r_2 (G_n^2 - G_n^2(0))], \end{aligned} \quad (2.28)$$

where

$$\begin{aligned} G_n^{-1} &= \beta_n [(d_n - d_{n-1})^2 - 1] + i(d_n - d_{n-1})(\tau_1 + \tau_2) - \beta_n^{-1}\tau_1\tau_2; \\ N \geq n = n_2 - n_1 + 1 \geq 1; \quad n_1 = 0, \quad 0 \leq \tau_1 < \infty; \quad n_2 = N - 1, \quad 0 \leq \tau_2 < \infty; \\ n_1 \geq 1, \quad 0 \leq \tau_1 \leq T; \quad n_2 \leq N - 2, \quad 0 \leq \tau_2 \leq T, \end{aligned} \quad (2.29)$$

here we used (2.22), (2.23) and (2.8). Note for the subtraction procedure one has that when $q \rightarrow 0$, the function b , $\beta_n \rightarrow \infty$.

The formula (2.28) can be rewritten in the form which is more convenient for application

$$\begin{aligned} \frac{dw_{br}^{(N)}}{d\omega} &= \frac{\alpha}{\pi\omega} \operatorname{Re} \int_0^\infty d\tau_2 \int_0^\infty d\tau_1 \exp[-i(\tau_1 + \tau_2 + \kappa T_1)] \\ &\times \left\{ \sum_{n=1}^{N-1} \exp[-i(n-1)\bar{\kappa}T] R_n(\tau_1, \tau_2) [\vartheta(T - \tau_1) + \vartheta(T - \tau_2) \right. \\ &\left. + (N - n - 1)\vartheta(T - \tau_1)\vartheta(T - \tau_2)] + \exp[-i(N-1)\bar{\kappa}T] R_N(\tau_1, \tau_2) \right\}, \end{aligned} \quad (2.30)$$

$$\text{where} \quad R_n(\tau_1, \tau_2) = r_1 (G_n - G_n(0)) + r_2 (G_n^2 - G_n^2(0)). \quad (2.31)$$

For one plate ($N = 1$) we have $n_1 = n_2 = 0$, $n = 1$ and

$$G_1^{-1} = i(\tau_1 + \tau_2) - \frac{1}{b}\tau_1\tau_2, \quad G_1^{-1}(0) = i(\tau_1 + \tau_2). \quad (2.32)$$

In the integral (2.28) we rotate the integration contours over τ_1, τ_2 on the angle $-\pi/2$ and substitute variables $\tau_{1,2} \rightarrow -ix_{1,2}$. Then we carry out change of variables $x = x_1 + x_2$, $x_2 = zx$. We have

$$\frac{dw_{br}^{(1)}}{d\omega} = \frac{\alpha}{\pi\omega} \cos\kappa T_1 \int_0^\infty \exp(-x) dx \int_0^1 \left[r_1 \left(1 - \frac{1}{g(x, z)} \right) \right] \quad (2.33)$$

$$\begin{aligned}
& +r_2 \left(1 - \frac{1}{g^2(x, z)} \right) \Big] dz = \frac{\alpha b}{\pi \omega} \cos(\kappa T_1) \int_0^\infty \exp(-bx) \\
& \times \left[r_1 F_1 \left(\sqrt{\frac{x}{4}} \right) + r_2 F_2 \left(\sqrt{\frac{x}{4}} \right) \right], \\
& g(x, z) = 1 + \frac{x}{b} z(1 - z), \quad F_1(u) = 1 - \frac{\ln(u + \sqrt{1 + u^2})}{u\sqrt{1 + u^2}}, \\
& F_2(u) = \frac{1 + 2u^2}{u\sqrt{1 + u^2}} \ln(u + \sqrt{1 + u^2}) - 1.
\end{aligned}$$

Here the integration by parts is carried out in the term $\propto r_2$ first over x and then over z in the term containing $\ln(1 + xz(1 - z))$. The expression (2.34) was derived in [7], Sect.5 (see also references therein) with allowance for the correction term $v(\mathbf{q})$ (see Eq.(2.13)).

We handle now to the case when a target consists of two plates ($N = 2$). Since the formation length is enough long for the soft photons ($\omega \ll \varepsilon$) only, we consider the term with r_2 in (2.28) as far as $r_1 = \omega^2/\varepsilon^2 \ll 1$. For the case ($N = 2$) the sum in (2.28) consists of three terms: 1) $n_1 = n_2 = 0$; 2) $n_1 = n_2 = 1$; 3) $n_1 = 0, n_2 = 1$. For the two first $n = 1$ and we have from (2.32)

$$\begin{aligned}
\frac{dw_{br1}^{(2)}}{d\omega} &= \frac{dw_{br2}^{(2)}}{d\omega} = \frac{\alpha r_2}{\pi \omega} \operatorname{Re} \left[\exp(-i\kappa T_1) \int_0^\infty d\tau_2 \int_0^T \exp(-i(\tau_1 + \tau_2)) \right. \\
& \times \left. \left[\frac{1}{(\tau_1 + \tau_2)^2} - \frac{1}{(\tau_1 + \tau_2 + i\tau_1\tau_2/b)^2} \right] d\tau_1 \right]. \tag{2.34}
\end{aligned}$$

For the third term $n = 2$, $d_2 = 2\alpha$ (see (2.18)) and we have

$$\begin{aligned}
G_2^{-1} &= iT + i \left(1 + \frac{iT}{b} \right) (\tau_1 + \tau_2) - \frac{2}{b} \left(1 + \frac{iT}{2b} \right) \tau_1 \tau_2 \\
&= i(T + \tau_1 + \tau_2) - \frac{2}{b} \tau_1 \tau_2 + \frac{iT}{b} \left[i(\tau_1 + \tau_2) - \frac{\tau_1 \tau_2}{b} \right], \tag{2.35}
\end{aligned}$$

so that

$$\begin{aligned} \frac{dw_{br3}^{(2)}}{d\omega} &= \frac{\alpha r_2}{\pi\omega} \operatorname{Re} \left[\exp(-i(\kappa T + \kappa T_1)) \int_0^\infty dx_1 \right. \\ &\times \int_0^\infty \exp(-(x_1 + x_2)) \left[\frac{1}{(iT + x_1 + x_2)^2} \right. \\ &\left. \left. - \frac{1}{[iT + x_1 + x_2 + \frac{2}{b}x_1x_2 + \frac{iT}{b}(x_1 + x_2 + \frac{x_1x_2}{b})]^2} \right] dx_2 \right]. \end{aligned} \quad (2.36)$$

Here we rotate the integration contours over τ_1, τ_2 on the angle $-\pi/2$ and substitute variables $\tau_{1,2} \rightarrow -ix_{1,2}$.

In the case of the weak multiple scattering ($b \gg 1$) neglecting the effect of the polarization of a medium ($\kappa = 1$) and expanding the integrand in (2.34) and (2.37) over $1/b$ we have for the probability of radiation

$$\begin{aligned} \frac{dw_{br}^{(2)}}{d\omega} &= 2 \frac{dw_{br1}^{(2)}}{d\omega} + \frac{dw_{br3}^{(2)}}{d\omega} \simeq \frac{2\alpha r_2}{3\pi\omega b} \left[1 - \frac{3}{10b} + \frac{1}{b}G(T) \right], \\ G(T) &= T^2 \int_0^\infty \frac{x^3 \exp(-x)}{(x^2 + T^2)^2} \left[\left(1 - \frac{3x^2}{10T^2} \right) \cos \left(T - 4 \arctan \frac{x}{T} \right) \right. \\ &\left. + \frac{2x}{T} \sin \left(T - 4 \arctan \frac{x}{T} \right) \right]. \end{aligned} \quad (2.37)$$

If the distance between plates is small ($T \ll 1$) we have

$$G(T) \simeq -\frac{3}{10} + 12T^2 \left(\ln \frac{1}{T} - C - \frac{19}{24} \right). \quad (2.38)$$

In the opposite case ($T \gg 1$) one can obtain asymptotic expansion of $G(T)$ using the method of stationary phase (similar method was used in derivation of the Stirling formula)

$$G(T) \simeq \frac{6T^2}{(9 + T^2)^2} \cos \left(T - 4 \arctan \frac{3}{T} \right) + \frac{48T}{(16 + T^2)^2} \sin \left(T - 4 \arctan \frac{4}{T} \right). \quad (2.39)$$

Note that the main term of the decomposition in Eq.(2.37) is the Bethe-Heitler probability of radiation from two plates which is independent of the distance between plates. This means that in the case considered we have independent radiation from each plate without interference in the main order over $1/b$. The interference effects appear only in the next orders over $1/b$.

In the case of the strong multiple scattering ($b \ll 1$, $p_c^2 \gg 1$) we consider first the transition region from $T \ll b$ (the formation length is much longer than the distance between plates) to $T \gg b$ (at small T , $T \ll 1$). We introduce parameter $\delta = iT/b$, then assuming $b \ll 1$, $T \ll 1$ we obtain

$$\begin{aligned}\frac{dw_{br1}^{(2)}}{d\omega} &= \frac{dw_{br2}^{(2)}}{d\omega} = \frac{\alpha r_2}{\pi\omega} \operatorname{Re} \left[\exp(-i\kappa T_1) f_1(\delta) \right], \\ \frac{dw_{br3}^{(2)}}{d\omega} &= \frac{\alpha r_2}{\pi\omega} \operatorname{Re} \left[\exp(-2i\kappa T_1) f_2(\delta) \right],\end{aligned}\quad (2.40)$$

where

$$\begin{aligned}f_1(\delta) &= (1+b) \ln(1+\delta) + \frac{b\delta^2}{1+\delta} (\ln(b\delta) + C - 1) + b\delta \left(\frac{\ln(1+\delta)}{1+\delta} - 1 \right), \\ f_2(\delta) &= \ln \left(\frac{2+\delta}{b(1+\delta)^2} \right) - 1 - C + b \left[\ln \left(\frac{2+\delta}{b(1+\delta)} \right) + 1 - C \right] \\ &\quad - \frac{b\delta}{1+\delta} [(1+2\delta) (\ln(b\delta) + C) + \ln(1+\delta) - \delta] \\ &\quad + \frac{b\delta}{(1+\delta)(2+\delta)} \ln \left(\frac{b\delta(1+\delta)}{2+\delta} \right).\end{aligned}\quad (2.41)$$

When the formation length is much larger than the target thickness as a whole ($T \ll b$, $|\delta| \ll 1$), one can decompose the functions $f_1(\delta)$ and $f_2(\delta)$ into the Taylor series over δ . Retaining the main terms of the expansion we find for the probability of radiation

$$\frac{dw_{br}^{(2)}}{d\omega} \simeq \frac{\alpha r_2}{\pi\omega} \left[(1+b) \left(\ln \frac{2}{b} + 1 - C \right) - 2 \right] \cos(2\kappa T_1) \quad (2.42)$$

In the opposite case $b \ll T \ll 1$ ($|\delta| \gg 1$) neglecting the effect of the polarization of a medium ($\kappa T_1 \ll 1$) we have

$$\frac{dw_{br}^{(2)}}{d\omega} \simeq \frac{\alpha r_2}{\pi\omega} \left[(1+2b) \left(\ln \frac{T}{b^2} + 1 - C \right) - 2 \right] \quad (2.43)$$

Note that when $T = 1$ the probability (2.43) is within logarithmic accuracy doubled probability of radiation from one plate with the thickness l_1 :

$$\frac{dw_{br}^{(1)}}{d\omega} \simeq \frac{\alpha r_2}{\pi\omega} \left[(1+2b) \left(\ln \frac{1}{b} + 1 - C \right) - 2 \right] \quad (2.44)$$

The case of the strong multiple scattering ($b \ll 1$) for the photon energies where the value $T \geq 1$ is of the special interest. In this case we can neglect the polarization of a medium $\kappa = \bar{\kappa} = 1$, and disregard the terms $\propto \kappa T_1$ in the exponent of the expressions (2.34) and (2.37) since $T_1 \ll 1$. In the integral over τ_1 in (2.34) we add and subtract the contribution of the interval $T \leq \tau_1 < \infty$. The sum gives Eq.(2.34), i.e. the radiation from one plate, and in the difference the main contribution gives region $\tau_2 \sim 1$ so that one can disregard the second terms in the square brackets in Eqs.(2.34) and (2.37). We obtain as a result

$$\begin{aligned} \frac{dw_{br}^{(2)}}{d\omega} &= 2 \frac{dw_{br1}^{(2)}}{d\omega} + \frac{dw_{br3}^{(2)}}{d\omega} \simeq 2 \frac{dw_{br}^{(2)}}{d\omega} - \frac{dw_{br3}^{(2)}}{d\omega}, \quad \frac{dw_{br3}^{(2)}}{d\omega} = \frac{\alpha r_2}{\pi \omega} F(T), \\ \text{Re } F(T) &= \int_0^\infty d\tau_2 \int_T^\infty d\tau_1 \frac{1}{(\tau_1 + \tau_2)^2} \exp(-i(\tau_1 + \tau_2)) \\ &= \int_T^\infty \frac{d\tau}{\tau^2} \exp(-i\tau)(\tau - T) = -(\text{ci}(T) + T \text{si}(T) + \cos T), \end{aligned} \quad (2.45)$$

where $\text{si}(z)$ is the integral sine and $\text{ci}(z)$ is the integral cosine. At $T \gg 1$ we have

$$F(T) = -\frac{\cos T}{T^2}. \quad (2.46)$$

We carried out the analysis of cases $N = 1, 2$ using Eq.(2.28). We illustrate an application of Eq.(2.31) for the case $N = 4$:

$$\begin{aligned} \frac{dw_{br}^{(4)}}{d\omega} &= \frac{\alpha}{\pi \omega} \text{Re} \left\{ \exp(-i\kappa T_1) \left[2 \int_0^\infty d\tau_2 \int_0^T d\tau_1 \exp[-i(\tau_1 + \tau_2)] \right. \right. \\ &\times \left(R_1 + \exp(-i\bar{\kappa} T) R_2 + \exp(-2i\bar{\kappa} T) R_3 \right) + \int_0^T d\tau_2 \int_0^T d\tau_1 \exp[-i(\tau_1 + \tau_2)] \\ &\left. \left. (2R_1 + \exp(-i\bar{\kappa} T) R_2) + \exp(-i3\bar{\kappa} T) \int_0^\infty d\tau_2 \int_0^\infty d\tau_1 \exp[-i(\tau_1 + \tau_2)] R_4 \right] \right\}. \end{aligned} \quad (2.47)$$

We consider now the case of large N ($N \geq 3$). If the formation length of the bremsstrahlung is shorter than the distance between plates ($T > 1$) the interference of the radiation from neighboring plates takes place. Using the probability of radiation from two plates (2.37) we obtain in the case of weak multiple scattering ($b \gg 1$)

$$\frac{dw_{br}^{(N)}}{d\omega} \simeq \frac{N\alpha r_2}{3\pi\omega b} \left[1 - \frac{3}{10b} + 2 \frac{N-1}{Nb} G(T) \right], \quad (2.48)$$

where for $T \gg 1$ the function $G(T)$ is defined in (2.37). In the case of strong multiple scattering ($b \ll 1$) and large T we have (compare with Eqs.(2.45) and (2.46))

$$\frac{dw_{br}^{(N)}}{d\omega} \simeq N \left(\frac{dw_{br}^{(1)}}{d\omega} + \frac{\alpha r_2}{\pi \omega b} \frac{N-1}{Nb} \frac{\cos T}{T^2} \right). \quad (2.49)$$

In the opposite limiting case $|\eta| \ll 1$, ($\eta^2 \simeq \delta$) $N|\eta| \ll 1$ (see Eqs.(2.20) and (2.21)), i.e. when the formation length of the bremsstrahlung is longer than the radiator thickness, the radiation act takes place on a target as a whole. In this case, as it follows from Eq. (2.21), the parameter b diminishes N times (the value p_c^2 increases N times). The analysis of the case of two plates conducted above in detail supports this result. In the limiting case of strong multiple scattering ($b \ll 1$) one can see this from (2.42).

In the case $|\eta| \ll 1$ (the formation length of the bremsstrahlung is longer than a distance between plates as before) and large N (including the case when $|N\eta| \gg 1$) one can substitute the summation over n by integration in the expression for the probability of radiation (2.28). Using Eqs.(2.19)-(2.22) we have

$$\begin{aligned} n\eta &\simeq nT2\sqrt{i\bar{q}} \rightarrow t\nu, & b\eta &\simeq \sqrt{ibT} = \frac{i}{2\sqrt{i\bar{q}}} = \frac{i}{\nu}, & d_n &\rightarrow \frac{\sinh \nu t}{\eta}, \\ \beta_n &\rightarrow \frac{b\eta}{\sinh \nu t} = \frac{i}{\nu \sinh \nu t}, & d_n - d_{n-1} &\rightarrow \cosh \nu t; \\ G_n^{-1} &\rightarrow \frac{i}{\nu} [\sinh \nu t + \nu (\tau_1 + \tau_2) \cosh \nu t + \nu^2 \tau_1 \tau_2 \sinh \nu t], \end{aligned} \quad (2.50)$$

where $\nu = 2\sqrt{i\bar{q}}$ (see [7], Sect.2). The four regions contribute into the sum and integrals over τ_1, τ_2 in Eq.(2.28), see also Eq.(2.31).

1. The first region $0 \leq \tau_1 < \infty$, $0 \leq \tau_2 \leq T$ ($\tau_1 \rightarrow t_1$, $nT \rightarrow t_2$), so we have in this region

$$G_n \rightarrow -iN_1, \quad N_1 \simeq \frac{\nu}{(\sinh \nu t_2 + \nu t_1 \cosh \nu t_2)},$$

where we take into account that $\nu T = \eta \ll 1$.

2. In the second region $0 \leq \tau_1, \tau_2 \leq T$ ($nT \rightarrow t_2 - t_1 = t$)

$$G_n \rightarrow -iN_2, \quad N_2 \simeq \frac{\nu}{\sinh \nu t}.$$

3. The third region gives the same contribution after substitution $\tau_1 \leftrightarrow \tau_2$, $t_1 \leftrightarrow t_2$.

4. In the fourth region $0 \leq \tau_1, \tau_2 < \infty$ ($\tau_{1,2} \rightarrow t_{1,2}$)

$$G_n \rightarrow -iN_4, \quad N_4 \simeq \frac{\nu}{(1 + \nu^2 t_1 t_2) \sinh \nu NT + \nu(t_1 + t_2) \cosh \nu NT}.$$

Substituting these expressions into Eq.(2.28) we arrive to the formula (2.11) of [8] which describes radiation on the plate of the thickness NT (in units of the formation length). This case was analyzed in detail in [8].

3 A qualitative analysis of the radiation in the structured target

We investigate the behavior of the spectral distribution $\omega \frac{dw}{d\omega}$ using as an example the case of two plates with the thickness l_1 and the distance between plates $l_2 \geq l_1$ which was analyzed in detail in the previous Section. For plates with the thickness $l_1 \geq 0.2\% L_{rad}$ and in the energy interval $\omega > \omega_p$, in which the effects of the polarization of a medium can be discarded, the condition (2.7) is fulfilled only for enough high energy ε , when the characteristic energy

$$\omega_c = \frac{16\pi Z^2 \alpha^2}{m^2} \gamma^2 n_a \ln \frac{a_s^2}{\lambda_c}, \quad (3.1)$$

where n_a is the number density of atoms in the medium, is such that $\omega_p \ll \omega_c$. We study the situation when the LPM suppression of the intensity of radiation takes place for relatively soft energies of photons: $\omega \leq \omega_c \ll \varepsilon$.

We consider first the hard photons $\omega_c \ll \omega < \varepsilon$. In this interval of ω the formation length l_0 (2.2) is much shorter than the plate thickness l_1 ($T_1 \gg 1$), the radiation intensity is the incoherent sum of radiation from two plates and it is independent of the distance between plates. In this interval the Bethe-Heitler formula is valid.

For $\omega \leq \omega_c$ the LPM effect turns on, but when $\omega = \omega_c$ the thickness of plate is still larger than the formation length l_0 (the opposite case will be considered in the end of the Section)

$$\frac{l_1}{l_0(\omega_c)} = T_1(\omega_c) \equiv T_c \simeq \frac{2\pi}{\alpha} \frac{l_1}{L_{rad}} > 1, \quad (3.2)$$

so that the formation of radiation takes place mainly inside each of plates. With ω decreasing we get over to the region where the formation length $l_c > l_1$, but effects of the polarization of a medium are still weak

($\omega > \omega_p$). Within this interval (for $\omega < \omega_{th}$) the main condition (2.6) is fulfilled. To estimate the value ω_{th} we have to take into account the characteristic radiation angles (p_c^2 in Eq.(2.6)), connected with mean square angle of the multiple scattering. Using Eq.(2.14) and the definition of the parameter $b = 1/(4qT_1)$ in Eq.(2.15)) we find

$$p_c^2 \leq \frac{1}{b} = \frac{2\pi}{\alpha} \frac{l_1}{L_{rad}} \left(1 - \frac{\ln \varrho_b}{\ln(a_{s2}/\lambda_c)} \right) \simeq T_c \left(1 + \frac{\ln T_c}{2 \ln(a_{s2}/\lambda_c)} \right);$$

$$\omega_{th} = \frac{\omega_c}{T_c(1+p_c^2)} \geq \omega_b = \frac{\omega_c}{T_c(1+T_c)}. \quad (3.3)$$

It is shown in [8] (Sec.3, see discussion after Eq.(3.6)) that $\omega_{th} \simeq 4\omega_b$ (in [8] the notation ω_2 was used instead of ω_b). Naturally, $\omega_{th} < \omega_c/T_c$, and when $\omega = \omega_c/T_c$ one has $T_1 = 1$, $l_1 = l_0$. It is seen from Eq.(3.3) that when the value l_1 decreases, the region of applicability of results of this paper grows.

So, when $\omega < \omega_{th}$ the formation length is longer than the thickness of the plate l_1 and the coherent effects depending on the distance between plates l_2 turn on. For the description of these effects for $T = (1 + l_2/l_1) T_1 \geq 1$ one can use Eq.(2.45). For $T \geq \pi \gg 1$ one can use the asymptotic expansion (2.46) and it is seen that at $T = \pi$ the spectral curve has minimum. Let us note an accuracy of formulas is better when ω decreases, and the description is more accurate for $T \gg T_1$ ($l_2 \gg l_1$).

With further decreasing of the photon energy ω the value T diminishes and the spectral curve grows until $T \sim 1$. When $T < 1$ the spectral curve decreases $\propto \ln T$ according with the second formula of Eq.(2.44). So, the spectral curve has maximum for $T \sim 1$. The mentioned decreasing continues until the photon energy ω for which $(1 + 2/b)T \sim 1$. For smaller ω the thickness of the target is shorter than the formation length. In this case the first Eq.(2.44) is valid which is independent of the value T .

The next characteristic region of the photon energies is $\omega \leq \omega_p$ where the polarization of a medium is manifest itself. For $\omega \sim \omega_0^2 l_1 \ll \omega_p$ one has $\kappa T_1 \sim 1$ and for the bremsstrahlung contribution instead of Eq.(2.44) we have to use Eqs.(2.42)-(2.43) which include the interference of the bremsstrahlung on the plate boundaries. However, in this region the transition radiation gives the main contribution.

The spectral probability of transition radiation in the radiator consisting of N thin plates of the thickness l_1 separated by equal distances l_2 was discussed in many papers, see e.g. [3]. It has the form

$$\frac{dw_{tr}^{(N)}}{d\omega} = \frac{4\alpha}{\pi\omega} \int_0^\infty \frac{ydy}{(1+y)^2} \left(\frac{\kappa_0^2}{(1+\kappa_0^2+y)} \right)^2 \Phi_N(y), \quad (3.4)$$

where

$$\Phi_N(y) = \sin^2 \frac{\varphi_1}{2} \frac{\sin^2(N\varphi/2)}{\sin^2(\varphi/2)}, \quad (3.5)$$

here $y = \vartheta^2 \gamma^2$, ϑ is the angle of emission with respect velocity of the incident electron (we assume normal incidence) and

$$\begin{aligned} \varphi_1 &= \frac{\omega l_1}{2\gamma^2} (1 + \kappa_0^2 + y) \simeq T_1(\kappa + y), \\ \varphi &= \frac{\omega l}{2\gamma^2} (1 + y) + \frac{\omega l_1}{2\gamma^2} \kappa_0^2 \simeq T(1 + y) + \kappa T_1 \end{aligned} \quad (3.6)$$

The formula (3.4) can be derived directly from Eq.(2.25) if one gets over to the p -representation (make

$$\int d^2 p |\mathbf{p} \rangle \langle \mathbf{p}|, \quad | \langle \mathbf{p}|0 \rangle |^2 = \frac{1}{(2\pi)^2},$$

than one substitutes the real part of the double integral over time by one-half of the modulus squared of the single integral. After substitution $\mathbf{p}^2 = y$, $d^2 p = \pi dp^2 = \pi dy$ we pass to Eq.(3.4).

In the case $N = 2$ one has

$$\Phi_2(y) = 4 \sin^2 \frac{\varphi_1}{2} \cos^2 \frac{\varphi}{2}. \quad (3.7)$$

In the integral in (3.4) for $y < 2/T \gg 1$ the function $\Phi_2 \simeq \sin^2 \kappa T_1$ and in the interval $\kappa \geq y > 2/T$ we can substitute $\cos^2 \varphi/2$ by its mean value $1/2$. As a result we have within logarithmic accuracy

$$\begin{aligned} F_2 &= \int_0^\infty \frac{y dy}{(1+y)^2} \left(\frac{\kappa_0^2}{(1+\kappa_0^2+y)} \right)^2 \Phi_2(y) \simeq \int_1^\kappa \frac{dy}{y} \Phi_2(y) \\ &\simeq \sin^2 \kappa T_1 \ln \frac{2}{T} + 2 \sin^2 \frac{\kappa T_1}{2} \ln \frac{\kappa T}{2} \vartheta (\kappa T - 1). \end{aligned} \quad (3.8)$$

The function F_2 vanishes in the points $\kappa T_1 \simeq \kappa_0^2 T_1 = 2\pi n$, the corresponding photon energies are

$$\omega_{(2n)} = \frac{\omega_0^2 l_1}{4\pi n} \equiv \frac{\omega_1}{n}, \quad \omega_1 = \frac{T_c \omega_p^2}{2\pi \omega_c}, \quad n = 1, 2, \dots \quad (3.9)$$

In the points $\kappa T_1 \simeq \pi(2n+1)$ the function F_2 has minimums which depend on the distance between plates l_2

$$\omega_{(2n+1)} \simeq \frac{2\omega_1}{2n+1},$$

$$F_2 \simeq 2 \ln \frac{\kappa T}{2} = 2 \ln \left(\frac{\kappa T_1}{2} \frac{l}{l_1} \right) \simeq 2 \ln \left[\left(n + \frac{1}{2} \right) \pi \frac{l}{l_1} \right], \quad l = l_1 + l_2 \quad (3.10)$$

The function F_2 has maximums in the points where $\sin \kappa T_1 \simeq 1$ ($\kappa T_1 \simeq \pi(m + 1/2)$) and in these points

$$\omega^{(m)} \simeq \frac{4\omega_1}{2m+1}, \quad F_2 \simeq \ln \kappa, \quad (3.11)$$

i.e. as the values of the function F_2 as well as the positions of the maximums of F_2 are independent of the distance between plates in the wide interval $l_2 \geq l_1$.

Now we perform similar analysis for arbitrary N . In the region $y < 2/(NT) \gg 1$ one has

$$\Phi_N \simeq \sin^2 \frac{N\kappa T_1}{2},$$

and in the interval $\kappa > y > 2/T$ the phase φ varies fast and the function

$$\frac{\sin^2(N\varphi/2)}{\sin^2(\varphi/2)} = |1 + \exp(-i\varphi) + \exp(-2i\varphi) + \dots|^2$$

can be substituted by its mean value N . In this interval $\Phi_N \simeq N \sin^2(\kappa T_1/2)$. In the intermediate region $2/T > y > 2/(NT)$ the phases φ_1 and φ are approximately equal and the function $\Phi_N \simeq \sin^2(N\varphi/2)$ oscillates fast and can be substituted by its mean value $1/2$. Taking this results into account we find performing the integration over y

$$\begin{aligned} F_N &= \int_0^\infty \frac{y dy}{(1+y)^2} \left(\frac{\kappa-1}{\kappa+y} \right)^2 \Phi_N(y) \simeq \int_1^\kappa \frac{dy}{y} \Phi_N(y) \\ &\simeq \sin^2 \frac{N\kappa T_1}{2} \ln \frac{2}{NT} + \frac{1}{2} \ln N + N \sin^2 \frac{\kappa T_1}{2} \ln \frac{\kappa T}{2}. \end{aligned} \quad (3.12)$$

It follows from this formula that positions of the minimums in the points $\omega = \omega_{(2n)}$ are independent of N , while the minimums in the points $\omega = \omega_{(2n+1)}$ are disappearing when the value N increases and for enough large N the function F_N has maximums in this points. The case $N \gg 1$ was considered in detail in our recent paper [14].

We will discuss now the results of numerical calculations given in Figs.1,2. The formulas (2.34), (2.37) and (3.4), (3.5) were used respectively. The spectral curves of energy loss were obtained for the case of two gold plates with the thickness $l_1 = 11.5 \mu m$ with different gaps l_2 between plates. The

initial energy of electrons is 25 GeV. The characteristic parameters for this case are:

$$\begin{aligned} \omega_c &\simeq 240 \text{ MeV}, & T_c &\simeq 2.9, & b^{-1} &\simeq 3.3, & \omega_{th} &\simeq 80 \text{ MeV}, \\ \omega_p &\simeq 3.9 \text{ MeV}, & \omega_1 &\simeq 30 \text{ keV}, & \frac{T}{T_1} &\equiv k = \frac{l_1 + l_2}{l_1} &= 3, 5, 7, 9, 11. \end{aligned} \quad (3.13)$$

At $\omega > 80$ MeV the radiation process occurs independently from each plate according with theory of the LPM effect [8]. The interference pattern appears at $\omega < 80$ MeV where the formation length is longer than the thickness of one plate and the radiation process depends on the distance between plates T . According to Eqs.(2.46), (2.48) the curves 1-5 have minimums at $\omega \simeq \pi\omega_{th}/k$ ($T = \pi$) which are outside of Fig.1 and will be discussed below. In accord with the above analysis the spectral curves in Fig.1 have the maximums at photon energies $\omega \simeq \omega_{th}/k$ ($T = 1$). These values (in MeV) are $\omega \simeq 27, 16, 11, 9, 7$ for curves 1, 2, 3, 4, 5 respectively. At further decrease of $\omega(T)$ the spectral curves diminish according to Eq.(2.44) and attain the minimum at $\omega_{min} = \omega_{th}/(k(1 + 2/b))$ ($T(1 + 2/b) = 1$). The corresponding values (in MeV) are $\omega \simeq 3.5, 2, 1.4, 1.2$ for curves 1, 2, 3, 4. The least value of $\omega_{min} \simeq 1$ MeV has the curve 5. However, one has to take into account that at $\omega \leq 1.5$ MeV ($\kappa_0^2 = p_c^2 \simeq 2/b$) the contribution of the transition radiation becomes significant. Starting from $\omega \leq 0.6$ MeV the contribution of the transition radiation dominates. The spectral curves for the transition radiation in Fig.2 increase for $\omega < 0.2$ MeV as $(\kappa T_1)^2 \ln 2/T$ ($\kappa T_1 \ll 1$) according to Eq.(3.8) and attain the maximal value at $\omega^{(0)} = 4\omega_1 = 0.12$ MeV (see Eq.(3.11)). The height of the spectral curves at this point within the logarithmic accuracy is independent of T and roughly the same for all the curves. The minimums of the spectral curves are disposed at $\omega_{(1)} = 2\omega_1 \simeq 0.06$ MeV according to Eq.(3.10) from which it follows that in this point for larger T the spectral curve is higher. The next maximum is situated in $\omega^{(1)} = 4\omega_1/3 = 0.04$ MeV. At $\omega_{(2)} = \omega_1 = 0.03$ MeV the spectral curves have the absolute minimum according to Eq.(3.8). At further decrease of ω the higher harmonics appear: maximum at the point $\omega^{(2)} = 4\omega_1/5 = 0.024$ MeV, the minimum at $\omega_{(3)} = 2\omega_1/3 = 0.02$ MeV etc.

The approach developed in this paper is applicable in the interval of photon energies where effects of the polarization of a medium are essential. It includes also the soft part of the LPM effect. For the case given in Fig.1 our results are given up to $\omega_{max} \sim 20$ MeV. On the other hand, in [13] the hard part of the LPM effect spectrum was analyzed where one can neglect the effects of the polarization of a medium ($\omega > 5$ MeV for the mentioned case). Although in our paper and in [13] the different methods are used, the

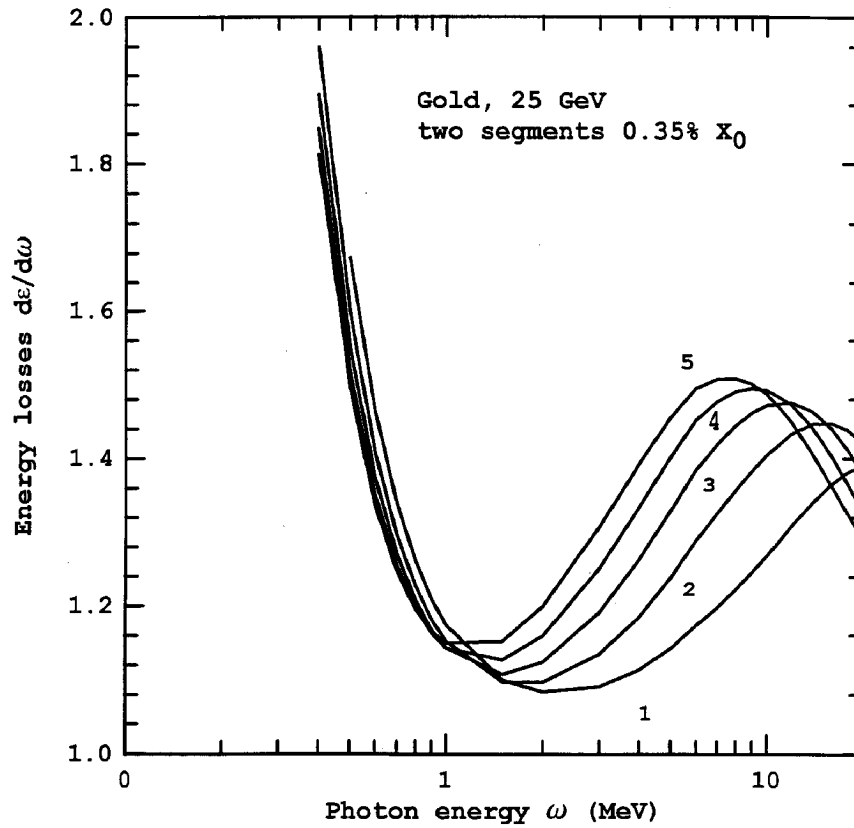


Figure 1: The energy losses spectrum $\frac{d\varepsilon}{d\omega}$ in units $\frac{2\alpha}{\pi}$, in the target consisting of two gold plates with thickness $l_1 = 11.5 \mu\text{m}$ for the initial electrons energy $\varepsilon=25 \text{ GeV}$:

- curve 1 is for distance between plates $l_2 = 2l_1$;
- curve 2 is for distance between plates $l_2 = 4l_1$;
- curve 3 is for distance between plates $l_2 = 6l_1$;
- curve 4 is for distance between plates $l_2 = 8l_1$;
- curve 5 is for distance between plates $l_2 = 10l_1$.

results obtained in overlapping regions are in a quite reasonable agreement among themselves.

It is interesting to discuss behavior of the spectral curves obtained in [13] from the point of view of our results. We consider the low value l_1 (T_c is not very large) and a situation when corrections to the value b in (3.3) which neglected in [13] are less than 20%. This leads to the difference in results less than 10%. We concentrate on the case of gold target with the total thickness $Nl_1 = 0.7\% L_{rad}$. The case $N = 1$ where $T_c = 5.8$, $b^{-1} = 7.3$, $\omega_c \simeq 240$ Mev, $\omega_{th} = 4\omega_c/(T_c(1 + T_c)) \simeq 24$ MeV is considered in detail in our paper [8]. The curves in figures in [13] are normalized on the Bethe-Heitler probability of radiation, i.e. they measured in units $\alpha r_2 T_c/(3\pi)$. In the region where our results are applicable $\omega < \omega_{th} \simeq 24$ MeV in Fig.2 ($G = 0$) of [13] one can see plateau the ordinate of which is 10% less than calculated according

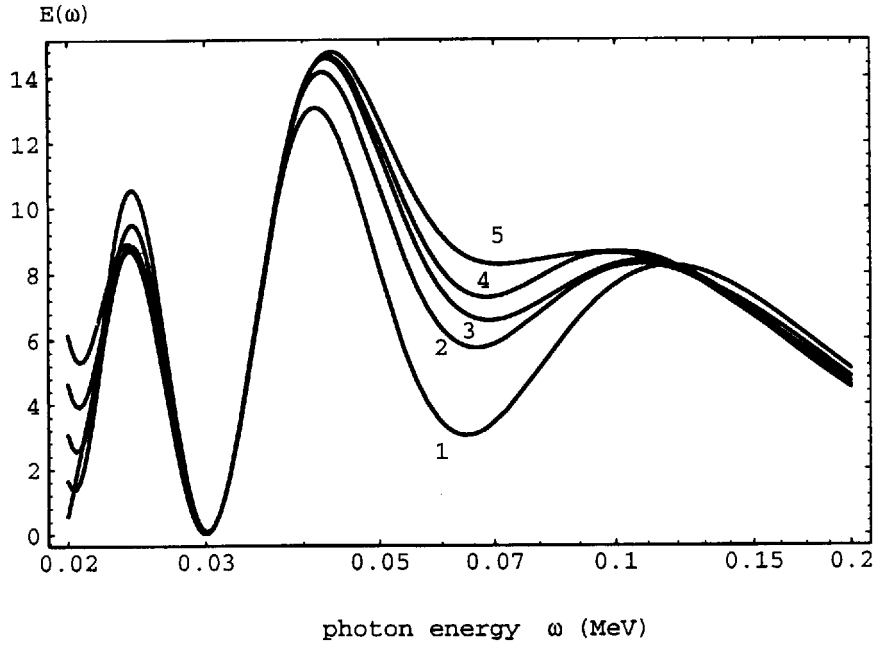


Figure 2: The same as in Fig.1 $E(\omega) = \frac{d\varepsilon}{d\omega}$ in soft part of the spectrum where transition radiation contributes only.

(2.34). The case of two plates ($T_c \simeq b^{-1} \simeq 3$, $\omega_c \simeq 240$ MeV, $\omega_{th} \simeq \omega_c/T_c = 80$ MeV) is given in Fig.3 of [13]. The lengths of the gaps are the same as in our Fig.1, except $k = 9$. The positions and ordinates of the minimums and the maximums in the characteristic points ($\omega \simeq \pi\omega_{th}/k$ for minimums and $\omega \simeq \omega_{th}/k$ ($T = 1$) for maximums, see above) as well as behavior of the spectral curves is described quite satisfactory by our formulas (see e.g. asymptotic Eqs.(2.42)-(2.46)).

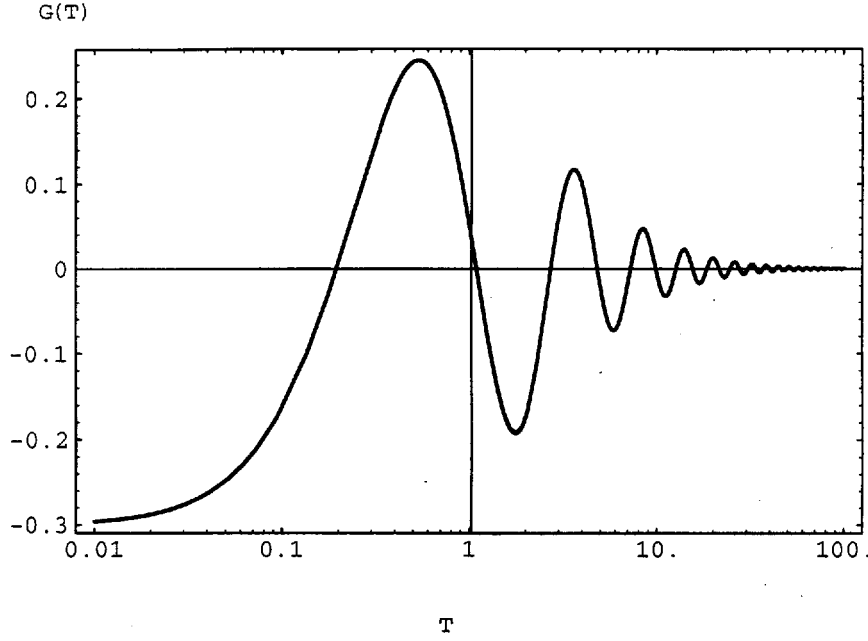


Figure 3: The function $G(T)$ (2.37).

In the case of four plates ($T_c \simeq b^{-1} \simeq 1.5$, $\omega_{th} \simeq \omega_c/T_c = 160$ MeV, Fig.4 of [13]) the value b is not enough small and we can do the qualitative analysis only. The curves in this figure correspond to the values $k = 3, 5, 9, 13$ according to Eqs.(2.42)-(2.46), (2.49). For $k = 13$ we have from (2.46): the first maximum is at $\omega \sim \omega_{th}/k \simeq 12$ MeV, the first minimum is at $\omega \sim \pi\omega_{th}/k \simeq 40$ MeV, the next maximum is at $\omega \sim 2\pi\omega_{th}/k \simeq 80$ MeV, the next minimum is at $\omega \sim 3\pi\omega_{th}/k \simeq 115$ MeV, but it is rather obscure because of large value of $T = 3\pi$. The accordance of these estimates of the

characteristic points with the curve in the figure is quite satisfactory.

Let us note in conclusion that for observation of the interference pattern at large values b which is described by Eq.(2.37) (see Fig.3) one needs to use very thin plates ($l_1 = \alpha L_{rad}/(2\pi b)$). Since the interference manifests itself in the terms $\propto 1/b$ only, the value b should not be very large. It seems at first sight that in this situation one can use the light elements, e.g. lithium, for which the radiation length L_{rad} is large. However, these elements have low charge of nucleus Z and low density and because of this the LPM effect begins at $\omega < \omega_c$ which is close to $\omega_p = \omega_0 \gamma$ where effects of the polarization of a medium are essential. So, one can expect that the optimal situation will be for elements in the middle of the periodic table of the elements. For example, for Ge one has $L_{rad} = 2.30$ cm, $\omega_0 = 44$ eV, and at energy $\varepsilon = 25$ GeV, $\omega_c = 34$ MeV, $\omega_{th} = b\omega_c = 100$ MeV, $\omega_p = 2.2$ MeV. Taking $b = 3$ we have $l_1 = 8.9$ μm , $\omega_1 = 6.95$ keV. In this situation there is rather wide interval of photon energies $\omega_p < \omega < \omega_{th}$ where the interference can be observed.

If one wants to observe the interference pattern $G(T)$ given by Fig.3 in the wide interval of T : $T_{min} \leq T \leq T_{max}$, $T_{min} \ll 1$, $T_{max} \gg 1$, then one has to take into account that $\omega = \omega_{th} T_1 = \omega_{th} T/k$ ($k = 1 + l_2/l_1$). In this situation one has

$$\begin{aligned} \omega_{max} &= \frac{T_{max}\omega_{th}}{k} < \omega_{th}, & k > T_{max}, \\ \omega_{min} &= \frac{T_{min}\omega_{th}}{k} > \omega_p, & k < \frac{\omega_{th}}{\omega_p} T_{min}. \end{aligned} \quad (3.14)$$

Acceptable parameters are $T_{max} \sim 10$, $T_{min} \sim 1/5$. For $T > 10$ the amplitude of oscillation is very small, while for $T \geq 0.2$ we have very distinct first maximum. So we have $k \simeq l_2/l_1 \simeq 10$ for the case considered.

Acknowledgments

This work was supported in part by the Russian Fund of Basic Research under Grant 98-02-17866.

A Appendix

We start calculation of $g_n(\mathbf{p}', \mathbf{p})$ (2.16) with lower terms $n = 2, 3$. Direct application of formula of the type Eq.(2.15) can be written in the form

$$g_n(\mathbf{p}', \mathbf{p}) = \frac{b}{\pi d_n} \exp \left\{ -\frac{b}{d_n} [(\mathbf{p}'^2 + \mathbf{p}^2) (d_n - d_{n-1}) - 2\mathbf{p}\mathbf{p}'] \right\}, \quad (\text{A.1})$$

where d_1, d_2, d_3 are given by Eq.(2.18). For arbitrary n we will use the mathematical induction method. Let (A.1) is valid for n , than for $n + 1$ we have from definition (2.16)

$$g_{n+1}(\mathbf{p}', \mathbf{p}) = \left(\frac{b}{\pi}\right)^2 \frac{1}{d_n} \int \exp \left\{ -\frac{b}{d_n} [(\mathbf{p}'^2 + \mathbf{p}_n^2) (d_n - d_{n-1}) - 2\mathbf{p}_n \mathbf{p}'] \right\} \\ \times \exp \left[-b (\mathbf{p}_n - \mathbf{p})^2 - i\mathbf{p}_n^2 T \right] d^2 p_n. \quad (\text{A.2})$$

The integral here is of the type Eq.(2.15), so we have

$$g_{n+1}(\mathbf{p}', \mathbf{p}) = \frac{b}{\pi d_n} \frac{b}{\beta_{n+1}} \exp \left(\frac{\alpha_n^2}{4\beta_{n+1}} \right) \exp \left[-\frac{b}{d_n} (d_n - d_{n-1}) \mathbf{p}'^2 - b\mathbf{p}^2 \right], \quad (\text{A.3})$$

where

$$\beta_{n+1} = b \left(\frac{d_n - d_{n-1}}{d_n} + 2\alpha - 1 \right), \quad \alpha_n^2 = 4b^2 \left(\frac{\mathbf{p}'^2}{d_n^2} + 2\frac{\mathbf{p}\mathbf{p}'}{d_n} + \mathbf{p}^2 \right).$$

In order that formula (A.1) will be valid for $n + 1$ the following equalities have to be fulfilled (they obtained from comparison of expressions Eqs.(A.1) and (A.3) at corresponding combinations of momenta)

$$\beta_{n+1} = \frac{b}{d_n} d_{n+1}, \quad d_n^2 = 1 + d_{n-1} d_{n+1}, \quad d_{n+1} = 2\alpha d_n - d_{n-1}. \quad (\text{A.4})$$

We consider the recursion relation somewhat more general than the last relation (A.4):

$$D_{n+1} = aD_n - b^2 D_{n-1}, \quad (\text{A.5})$$

with the initial conditions $D_2 = a$, $D_3 = a^2 - b^2$. We will find the explicit form of D_n using Okunev's method. The quadratic equation $z^2 - az + b^2 = 0$

has the roots

$$z_1 = \frac{a}{2} + A, \quad z_2 = \frac{a}{2} - A, \quad A = \sqrt{\frac{a^2}{4} - b^2}. \quad (\text{A.6})$$

Substituting these roots into Eq.(A.5) we can write

$$D_{n+1} = (z_1 + z_2) D_n - z_1 z_2 D_{n-1}. \quad (\text{A.7})$$

From this relation we have

$$\begin{aligned} D_{n+1} - z_1 D_n &= z_2 (D_n - z_1 D_{n-1}) = \dots = z_2^{n-2} (D_3 - z_1 D_2), \\ D_{n+1} - z_2 D_n &= z_1 (D_n - z_2 D_{n-1}) = \dots = z_1^{n-2} (D_3 - z_2 D_2). \end{aligned} \quad (\text{A.8})$$

Multiplying the first relation by z_2 and the second relation by z_1 and subtracting one from another we obtain

$$\begin{aligned} D_{n+1} &= \frac{1}{2A} \left[\left(\frac{a}{2} + A \right)^{n-1} \left(a^2 - b^2 - a \left(\frac{a}{2} - A \right) \right) \right. \\ &\quad \left. - \left(\frac{a}{2} - A \right)^{n-1} \left(a^2 - b^2 - a \left(\frac{a}{2} + A \right) \right) \right] \\ &= \frac{1}{2A} \left[\left(\frac{a}{2} + A \right)^{n+1} - \left(\frac{a}{2} - A \right)^{n+1} \right], \end{aligned} \quad (\text{A.9})$$

where A is defined in Eq.(A.6). If $a = 2\alpha$, $b = 1$ we have from the last formula Eq.(2.17). The second recursion relation of Eq.(A.4) is also satisfied by Eq.(2.17).

Note that n -lines determinant

$$D_{n+1} = \begin{vmatrix} a & b & 0 & \cdots & 0 & 0 \\ b & a & b & \cdots & 0 & 0 \\ 0 & b & a & \cdots & 0 & 0 \\ \dots & \dots & \dots & \dots & \dots & \dots \\ 0 & 0 & 0 & \cdots & a & b \\ 0 & 0 & 0 & \cdots & b & a \end{vmatrix}$$

gives the recursion relation (A.5) and so Eq.(A.9) gives value of this determinant.

References

- [1] L. D. Landau and I. Ya. Pomeranchuk, Dokl.Akad.Nauk SSSR **92**, 535, 735 (1953). See in English in *The Collected Paper of L. D. Landau*, Pergamon Press, 1965.
- [2] A. B. Migdal, Phys. Rev. **103**, 1811 (1956).
- [3] M. L. Ter-Mikaelian, *High Energy Electromagnetic Processes in Condensed Media*, John Wiley & Sons, 1972.
- [4] P. L. Anthony, R. Becker-Szendy, P. E. Bosted *et al*, Phys. Rev. Lett. **75**, 1949 (1995).
- [5] P. L. Anthony, R. Becker-Szendy, P. E. Bosted *et al*, Phys. Rev. Lett. **76**, 3550 (1996).
- [6] P. L. Anthony, R. Becker-Szendy, P. E. Bosted *et al*, Phys.Rev. D **56**, 1373 (1997).
- [7] V. N. Baier and V. M. Katkov, Phys.Rev. D **57**, 3146 (1998).
- [8] V. N. Baier and V. M. Katkov, *The Landau-Pomeranchuk-Migdal effect in a thin target*, hep-ph 9712524, Preprint BINP 97-105, Novosibirsk, 1997. *Quantum Aspects of Beam Physics*, ed. P.Chen, World Scientific PC, Singapore, 1998, p.525.
- [9] V. N. Baier and V. M. Katkov, Phys.Rev.D **59**, 056003 (1999).
- [10] R.Blancnbeckler and S. D. Drell, Phys. Rev. D **53**, 6265 (1996).
- [11] R. Baier, Yu. L. Dokshitzer, A. H. Mueller, S. Peigne, and D. Schiff, Nucl. Phys. **B478**, 577 (1996).
- [12] S. Klein *Suppression of Bremsstrahlung and Pair Production due to Environmental Factors*, hep-ph 9802442, LBL-41350, Berkeley, 1998. (submitted to Rev. Mod. Phys.)
- [13] R.Blancnbeckler, Phys.Rev. D **55**, 190 (1997).
- [14] V. N. Baier and V. M. Katkov, *Transition radiation as a source of quasi-monochromatic X-rays*, hep-ex 9812028, Preprint BINP 98-91, Novosibirsk, 1998.